International Journal of Sciences

Research Article Volume 12 – June 2023 (06)

Islet Dysfunction Induced by Niemann-Pick C1 (*NPC1*) Heterozygous Mutation Combined with High-fat Diet in C57BL/6C Mice

Linhai Zou[1,2], Ji Zhou[1,2], Guohui Jiang[1], Lixia Ji[1]

[1]Department of Pharmacology, School of Pharmacy, Qingdao University, No. 13 Ningde Road, Shinan District, Qingdao, 266021, China
[2]These authors contributed equally

Running Head: Niemann-Pick C1 and islet dysfunction

Abstract: Male patients with *NPC1* heterozygous mutation (*Npc1*$^{+/-}$) are prone to obesity and diabetes, yet the mechanism remains unclear. In this study, male *Npc1*$^{+/-}$ mice (C57BL/6C-*Npc1*) were used to evaluate the effects of *NPC1* heterozygous mutation combined with 60% high-fat diet (HFD) on glucolipid metabolism, cholesterol accumulation, islet dysfunction and β-cell dedifferentiation. Compared with male HFD-*Npc1*$^{+/+}$ or *Npc1*$^{+/-}$ mice fed with low-fat diet (LFD), body weight of male HFD-*Npc1*$^{+/-}$ mice gradually increased with elevated levels of fasting blood glucose (FBG), total cholesterol (TC) and triglyceride (TG), showing hyperinsulinemia and typical characteristics of diabetes. Oral glucose tolerance test (OGTT) and insulin tolerance test (ITT) indicated that HFD-*Npc1*$^{+/-}$ mice developed marked oral glucose intolerance and severe systemic insulin resistance after 4 months. TC and TG were accumulated in both liver and pancreas. The HE results confirmed the large diameter of epididymal adipocytes in HFD-*Npc1*$^{+/-}$ mice. Furthermore, protein levels of insulin, 4E-BP1, p-S6 and PDX1 were suppressed obviously in β cells of HFD-*Npc1*$^{+/-}$ mice, while expression of glucagon and precursor marker ALDH1A3 increased, indicating the typical dedifferentiation occurred in β cells. This study partly reveals the underlying mechanism of susceptibility of obesity and diabetes in *Npc1*$^{+/-}$ male mice induced by 60% HFD. High metabolic stress and abnormal cholesterol metabolism in islets more directly lead to the dedifferentiation and dysfunction of β cells, to aggravate the process from obesity to diabetes.

Keywords: *NPC1*, Diabetes, Hyperglycemia, β-cells, Dedifferentiation

Introduction

Cholesterol can enter mammalian cells through receptor-mediated low-density lipoprotein (LDL) in plasma. Cholesterol ester (CE) is degraded by lysosomes, which binds to membrane transporters Niemann-Pick C2 (NPC2) and Niemann-Pick C1 (NPC1) successively, and is finally transported out of the cell [1]. The *NPC1* gene is located on chromosome 18, and encodes a complex membrane binding protein composed of 1278 amino acids. NPC1 protein contains 13 transmembrane helical domains and 3 large lumen domains, of which the N-terminal domain (NTD) and sterol sensitive domain (SSD) can bind to cholesterol independently and play a key role in lipid transport [2]. The above theories clarify the process of lipid transmembrane transport and deepen the understanding of Niemann-Pick C disease, which is a rare autosomal recessive lipid storage disorder caused by *NPC* gene mutation, and characterized by hepatosplenomegaly and progressive neurodegeneration [3, 4].

Previous studies have shown that 95% *NPC* disease are caused by loss of *NPC1* function, and only 5% are related to the dysfunction of *NPC2* [5-8]. A genome-wide association study (GWAS) based on European populations has revealed that obesity in European adults is partly associated with the mutation of *NPC1* gene [9, 10]. NPC1 protein plays a central role in maintaining lipid homeostasis by regulating the transport of lipoprotein-derived lipids (cholesterol and free fatty acids) from late endosomes / lysosomes to other cells [11]. However, the deletion of *NPC1* gene may lead to abnormal accumulation of intracellular cholesterol, further affect the physiological function [12].

Related studies on BALB/cJ mice with *Npc1* heterozygous mutation indicated the gene-food interaction, *NPC1* heterozygous mutation (*Npc1*$^{+/-}$) mice with loss of 50% *NPC1* gene sharply gained body weight when fed with high fat diet compared to *NPC1* homozygous (*Npc1*$^{+/+}$) mice [13, 14]. And subsequent findings showed BALB/cJ-C57BL/6J heterozygous mutant mice were more likely to be obese and glucose intolerant after HFD feeding [15, 16]. A clinical statistic showed that the body mass index of male patients with *NPC1* heterozygous mutation was significantly higher than that of the control group [17].

In order to further explore the combined effect of *Npc1*$^{+/-}$ and HFD on islet function, we hybridized *Npc1*$^{-/-}$ mice with wild-type C57BL/6J mice to establish the model of C57BL-*Npc1*$^{+/-}$ mice. It was found that male *Npc1*$^{+/-}$ mice were more sensitive to 60% HFD than female *Npc1*$^{+/-}$ and *Npc1*$^{+/+}$ mice. When these male *Npc1*$^{+/-}$ mice were fed with 60% HFD, the body weight gain increased markedly, characterized by hypertrophy of visceral adipocyte. These *Npc1*$^{+/-}$ mice also showed significant disorders of glucolipid metabolism, including elevated fasting blood glucose, glucose intolerance, impaired insulin sensitivity and dyslipidemia. Furthermore, we found that cholesterol accumulation in pancreas increased the workload of islets and aggravated the β-cell dedifferentiation and

Published at: http://www.ijsciences.com/pub/issue/2023-06/
DOI: 10.18483/ijSci.2685; Online ISSN: 2305-3925; Print ISSN: 2410-4477

Guohui Jiang, Lixia Ji (Correspondence)
+13370830026, 15063930201

dysfunction.

Materials and Methods

Materials

The normal C57BL/6C mice (18-22 g, 7 weeks) and *NPC1* knockout mice (C57BL/6C-*Npc1*$^{-/-}$) were used in this study. C57BL/6C mice were purchased from Vital River Laboratory Animal Technology (Beijing, China, license number: SCXK (J) 2021-0011), and C57BL/6C-*Npc1*$^{-/-}$ mice were donated by Ruijin Hospital, Shanghai, China. The experimental animals were placed in the Experimental Animal Center of Qingdao University (SPF standard) with adequate food and water. All animal protocols were implemented in accordance with the guidelines for the care and use of laboratory animals prepared and approved by the animal protection committee of Qingdao University.

Gene identification

Normal C57BL/6C mice were hybridized with C57BL/6C-*Npc1*$^{-/-}$ mice. The tails (1-2 mm) of offspring mice were degraded in hydrolysate and protease K (Sorabo, China). DNA was extracted by chloroform and amplified, and the genotypes of offspring mice were identified by agarose gel electrophoresis.

Experimental design

120 male mice (60 *Npc1*$^{+/+}$ and 60 *Npc1*$^{+/-}$ mice) and 12 female mice (6 *Npc1*$^{+/+}$ and 6 *Npc1*$^{+/-}$ mice) were obtained. After 6 weeks of adaptive feeding, mice of each group were fed with 6% LFD or 60% HFD, respectively. The body weight and food intake of mice were recorded once a week, and OGTT, ITT, FBG, TC and TG were detected at the for 2, 4 and 6 months. The operation of all animal experiments is in accordance with the ethical review guidelines for the welfare of experimental animals in Qingdao.

Biochemical analyses

Serum samples were collected after feeding LFD or HFD for 2, 4 and 6 months. Serum TC, TG, high density lipoprotein cholesterol (HDL-c) and low-density lipoprotein cholesterol (LDL-c) were detected by kits (Nanjing Jiancheng Technology Co., Ltd.). At the same time, the content of serum insulin was detected by insulin kit (American ALPCO mouse hypersensitive insulin ELISA kit). Then the liver and pancreas were grinded to obtain homogenate for the determination of TC and TG by the same method mentioned above.

Oral glucose tolerance test (OGTT) and insulin tolerance test (ITT)

After fasting for 4 hours, glucose solution (2g/kg) was given by intragastric administration. The blood glucose was measured before glucose-loading (0min) and at 30min, 60min and 120min after glucose loading. And the area under curve (AUC) is calculated by using the following formula, AUC=0.25* (S_0+S_{30}) + 0.25 * (S_{30}+S_{60}) + 0.5 (S_{60}+S_{120}).

After fasting for 4 hours, insulin solution (0.4U/kg) was injected subcutaneously, and the blood glucose at 0 min was measured before injection, then the blood glucose was measured at 40 and 90 min after injection. The percentage of blood glucose decrease at 40 min was calculated to be (S_0-S_{40}) / S_0 × 100%.

HE staining

Liver and pancreas were fixed in 4% paraformaldehyde for 24-48 hours and then embedded with paraffin after dehydration. The sections were stained with hematoxylin-eosin (Sorabo, China), and the morphological characteristics of liver and pancreas were observed and analyzed.

Quantitative real-time PCR

Total RNA was extracted from liver with Trizol reagent (Sigma-Aldrich). After reverse transcription, combined with primers, it was detected by Bio-Rad fluorescence quantitative instrument. β-actin was used as the internal control of data standardization. The target gene primers have been listed in Table 1.

Immunohistochemistry and immunofluorescence

Adipose tissue and pancreas were fixed with 4% paraformaldehyde and embedded in paraffin. The sections were dewaxed with xylene ethanol gradient, repaired with EDTA buffer, permeabilized with 0.1% Triton X-100, and then blocked with 0.5% BSA. Primary antibodies insulin (Abcam, ab282459; 1:1000), glucagon (Novus Biologicals, NBP2-21803F; 1:4000), PDX1 (Abcam, 1:300; ab219207) and ALDHA3 (Novus, 1:500; NBP2-15339) were used in turn at 4 ° C overnight, and then the A corresponding secondary antibodies (Goat anti-mouse IgG, donkey anti-rabbit IgG, 1:1000, Abcam) and Alexa fluor 488 anti-rabbit (Abcam, ab150077; 1:300), Alexa flow 488 anti-mouse (Abcam, ab150113; 1:300), Alexa flower 647 anti-rabbit (Abcam, ab150079; 1:300) was used to detect the primary antibody, and DAPI was used to detect the nucleus. Finally, confocal microscopy was performed (Nikon, Japan).

Statistical analyses.

All the experimental results were statistically analyzed with Graphpad prism 8.0, and the statistical data were expressed as mean ± SD. one-way ANOVA was used to analyze the data, and the significant difference ($P < 0.05$) was statistically significant.

Result

1. Identification of *Npc1*$^{+/-}$ mice

PCR technique was used to identify *Npc1*$^{+/-}$ mice. As shown in DNA electrophoresis of Fig.1A, the *Npc1*$^{+/-}$ mice had bands at 450 bp, while *NPC1* wild type mice (*Npc1*$^{+/+}$) had no bands at 450 bp.

2. Weight gain curve

Npc1$^{+/+}$ and *Npc1*$^{+/-}$ mice were fed with LFD or HFD for growth analysis to explore the effects of *NPC1* gene - diet interactions on body weight. The body weight of mice fed with LFD or HFD from week 6 to 28 were shown in Fig.1B. There was no significant difference in body weight between female *Npc1*$^{+/+}$ and *Npc1*$^{+/-}$ mice fed with HFD. In contrast, compared with male HFD-

Npc1$^{+/+}$ mice, body weight of male HFD-*Npc1*$^{+/-}$ mice significantly increased by 12.3% (35.8 ±3.3g vs. 31.88 ±1.5g). The white fat index (epididymal fat and abdominal fat) and liver index in male HFD-*Npc1*$^{+/-}$ mice were much higher than those of HFD-*Npc1*$^{+/+}$ mice (Fig.1C).

3. Pathological morphology of epididymal adipose tissue

HE staining was used to observe the morphology of epididymal adipose tissue of male *Npc1*$^{+/+}$ and *Npc1*$^{+/-}$ mice fed with LFD or HFD. The results showed that the diameters of epididymal adipocytes in LFD-*Npc1*$^{+/-}$ and LFD-*Npc1*$^{+/+}$ mice were similar (Fig.1D-E), but the diameter of epididymal adipocytes in HFD-*Npc1*$^{+/-}$ mice were marked larger than that of HFD-*Npc1*$^{+/+}$ or LFD-*Npc1*$^{+/-}$ mice, and the number of adipocytes in the same visual field under microscope was decreased. Therefore, when male *Npc1*$^{+/-}$ mice were fed with HFD, the amount and diameter of epididymal adipocytes increased obviously, the increased proportion of adipose tissue stored more energy, which further confirmed the correlation between *NPC1* gene and high calorie diet.

4. Analysis of lipid metabolism

4.1 Detection of HDL-c and LDL-c in serum

The levels of HDL-c and LDL-c in serum of LFD-*Npc1*$^{+/-}$ were higher than those of LFD-*Npc1*$^{+/+}$ mice in Fig.S1. In other two groups, serum HDL-c and LDL-c of HFD-*Npc1*$^{+/-}$ mice increased gradually compared with those of HFD-*Npc1*$^{+/+}$ mice from the 4th month, and showed significant difference at the end of 6 months. Therefore, *NPC1*$^{+/-}$ plus HFD can destroy the dynamic balance of lipid metabolism.

4.2. Detection of TC and TG in serum

As shown in Fig.S2, compared with LFD-*Npc1*$^{+/-}$, serum TC increased significantly in HFD-*Npc1*$^{+/-}$ mice after 2 months feeding. Subsequently, TC level of HFD-*Npc1*$^{+/-}$ group was much higher than that of LFD-*Npc1*$^{+/-}$ or HFD-*Npc1*$^{+/+}$ ($P < 0.0001$, $P < 0.01$). Then, it showed similar trend as that of TC. After 6 months, content of TG of HFD-*Npc1*$^{+/-}$ mice also increased, and it was markedly higher than that of other groups. Therefore, heterozygous mutation of *Npc1* gene causes abnormal accumulation of TC and TG under HFD feeding, leading to obvious hyperlipidemia.

5. Analysis of glucose metabolism

As shown in Fig.2A-C, the continuous changes of FBG were measured. After 2 months, the FBG of HFD-*Npc1*$^{+/-}$ was much higher than that of LFD-*Npc1*$^{+/-}$ mice ($P < 0.05$); and at the end of 6 months, the FBG of HFD-*Npc1*$^{+/-}$ mice was even much higher than that of HFD-*Npc1*$^{+/+}$ mice. As to the serum insulin concentration, there was no significant difference between LFD-*Npc1*$^{+/+}$ and LFD-*Npc1*$^{+/-}$ mice in the whole duration (Fig.2D-F); but it was significantly higher in HFD-*Npc1*$^{+/-}$ mice than that of LFD-*Npc1*$^{+/+}$ mice after 2 months, and the insulin level of HFD-*Npc1*$^{+/-}$ mice was 36.7% higher than that of HFD-*Npc1*$^{+/+}$ mice at the end of 6 months (5.21 ±0.4 nM vs. 3.81 ±0.5 nM, P <0.01) (Fig. 2F). Therefore, *Npc1*$^{+/-}$ gene plus 60% HFD can easily lead to hyperinsulinemia, suggesting that *NPC1* gene mutation is more prone to insulin resistance and hyperglycemia under high calorie diet.

6. Oral glucose tolerance

Results of OGTT showed that there was no significant difference in blood glucose value between LFD-*Npc1*$^{+/-}$ and LFD-*Npc1*$^{+/+}$ mice at each time-point in OGTT from 2 to 6 months (Fig.2G-I). However, compared with HFD-*Npc1*$^{+/+}$, blood glucose value of HFD-*Npc1*$^{+/-}$ mice increased gradually at each time-point after 2 months, and it increased by 37.3% at 0 min, by 16.1% at 30 min, by 27.7% at 60 min, by 27.8% at 120 min respectively at the end of 6 months. And AUC of HFD-*Npc1*$^{+/-}$ mice also showed the similar increasing trend. Therefore, *Npc1*$^{+/-}$ together with 60% HFD is closely related to abnormal oral glucose tolerance, indicating a decline in glucose homeostasis regulation.

7. Insulin resistance

During the continuous change of glucose blood value in ITT, we used the decline percentage of blood glucose at 40 min after insulin injection to evaluate the insulin sensitivity. As shown in Fig.2M-R, the decline percentage at 40 min of HFD-*Npc1*$^{+/-}$ mice after 2 months was significantly lower than that of LFD-*Npc1*$^{+/-}$ group ($P < 0.05$), the gap widened further in the next four months. At the end of 6 months, the decline percentage at 40 min of HFD-*Npc1*$^{+/-}$ group was markedly lower than that of LFD-*Npc1*$^{+/-}$ group ($P < 0.001$) or HFD-*Npc1*$^{+/+}$ group ($P < 0.05$). Therefore, when *NPC1* heterozygous mutants encounters over-nutrition, the systemic insulin sensitivity decreases, and the mutation of *Npc1* gene can increase the susceptibility to insulin resistance.

8. TC/ TG contents and inflammation in liver and pancreas

After 6-month feeding, the livers and pancreas were collected. The results of immunohistochemistry showed that the expression of NPC1 protein in liver and pancreas was decreased in both LDF-*Npc1*$^{+/-}$ and HDF-*Npc1*$^{+/-}$ groups (Fig.3A-B). Contents of TC and TG showed that there was no significant difference in liver and pancreas between LFD-*Npc1*$^{+/-}$ and LFD-*Npc1*$^{+/+}$ mice. In another two groups, the contents of TC and TG in HFD-*Npc1*$^{+/-}$ mice were markedly higher than those of HFD-*Npc1*$^{+/+}$ mice (Fig.3C-F). Subsequent HE staining showed that the liver fat infiltration was obvious and islet morphology was destroyed in HFD group (Fig.3G-H). We further examined the mRNA levels of inflammatory cytokines in liver, the expression of TNF-α and IL-1β in HFD-*Npc1*$^{+/-}$ mice was much higher than those in other groups (Fig.3I-J), indicating a inflammatory state in livers of HFD-*Npc1*$^{+/-}$ mice. Therefore, *Npc1*$^{+/-}$ combined with HFD in male mice can increase the accumulation of cholesterol in liver and pancreas, causing metabolic inflammation and fat infiltration, which are likely to interfere with the physiological function of liver and pancreas.

9. Activation of mTORC1 pathway in islets

The above experiments confirmed the accumulation of cholesterol in the pancreas, and it's also found that amyloid protein could not be detected in islets by sulfur S staining (Fig.S3). Next, we found that the expression of two key regulatory factors 4E-BP1 and p-S6 in islets were obviously decreased in HFD-*Npc1*$^{+/-}$ group (Fig.3K-L), mTORC1 signal pathway was partly suppressed, which may affect the differentiation and function of β cells.

10. Analysis of function and differentiation of islet β cells

By the immunofluorescence and immunohistochemistry, it was found that the expression of insulin and glucagon in LFD-*Npc1*$^{+/-}$ was similar to that of LFD-*Npc1*$^{+/+}$ mice. However, in another two groups fed with HFD, insulin expression decreased significantly and glucagon expression increased in islets of HFD-*Npc1*$^{+/-}$ mice compared with those of HFD-*Npc1*$^{+/+}$ mice (Fig.4). In addition, we found that expression of PDX1, an identity marker of β cells, was much lower in HFD-*Npc1*$^{+/-}$ mice than that of other groups, but expression of ALDH1A3 was significantly increased (Fig.4). ALDH1A3 is regarded as β-cell precursor marker, its upregulation can accelerate the dedifferentiation of β cells into precursors, and impair the islet function.

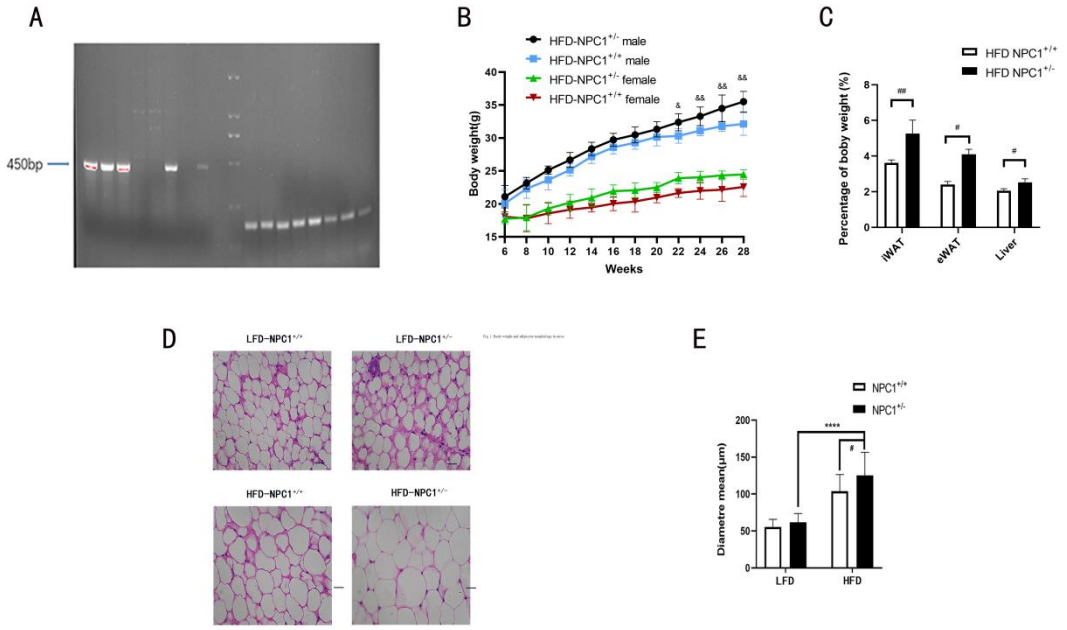

Fig. 1. Body weight and adipocyte morphology in

Fig. 1. Body weight and adipocyte morphology in mice. A. Identification of Npc1+/- mice by DNA electrophoresis; B. Body weight growth curve of male and female mice fed with 60% HFD; C. Oragan index of epididymal white adipose tissue(eWAT), inguinal white adipose tissue(iWAT) and liver in male mice fed with 60% HFD; D. HE staining of epididymal adipose tissue; E. The diameter of epididymal adipocytes. Data are presented as mean ± SEM, n=5-8. (&P<0.05, &&P<0.01 vs. HFD-*Npc1*$^{+/+}$ male; #P<0.05, ##<0.01 vs. HFD-*Npc1*$^{+/+}$ mice; *P < 0.05, **P < 0.01, ****P < 0.0001 vs. LFD-*Npc1*$^{+/-}$ mice;)

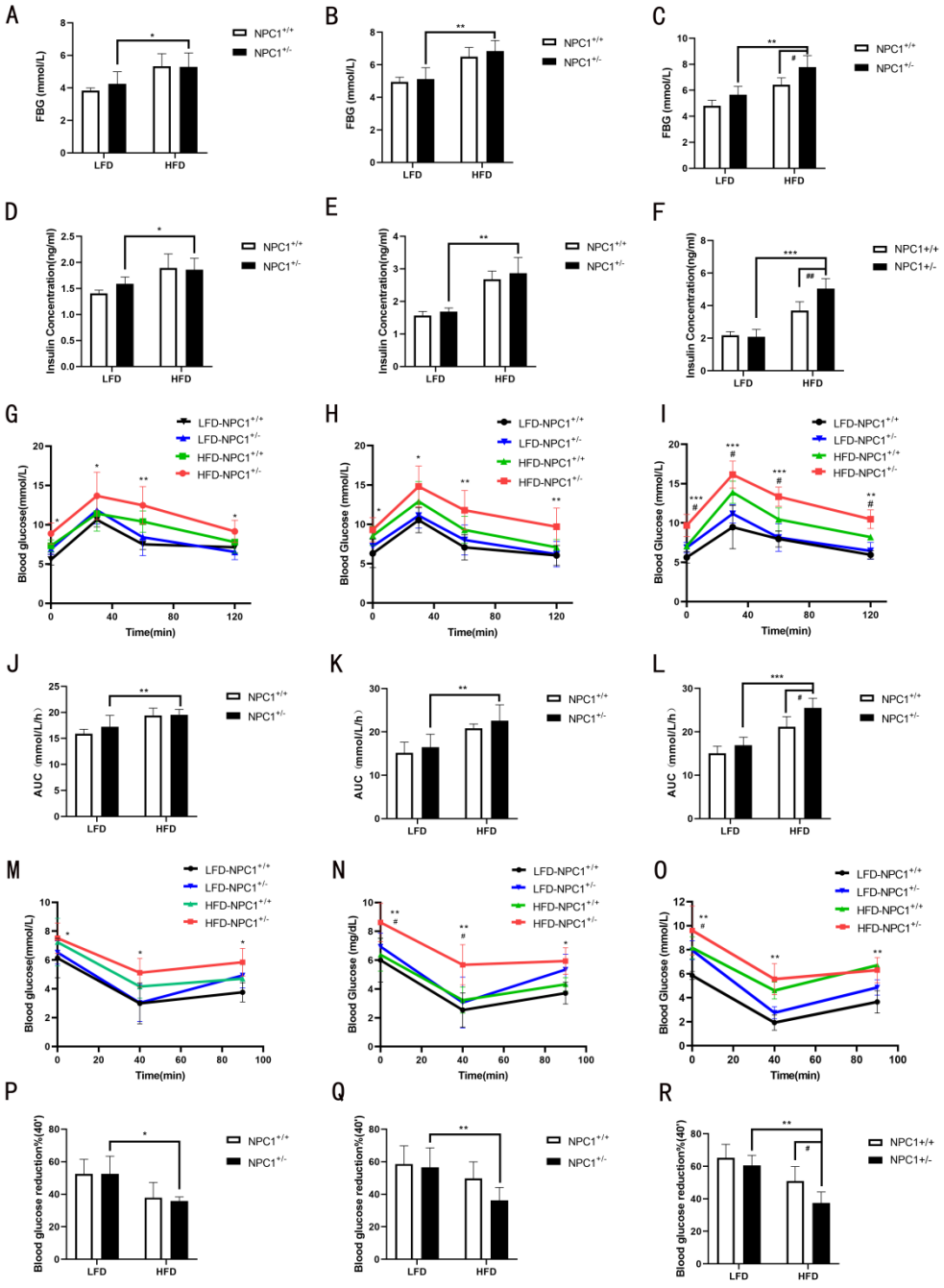

Fig 2. Changes of glucose metabolism and insulin sensitivity in mice.

Fig 2. Changes of glucose metabolism and insulin sensitivity in mice. A-C. FBG levels of each group at the end of 2, 4 and 6 months; D-F. Serum insulin levels; G-I. Blood glucose curves of OGTT; J-L. The area under curve (AUC) in OGTT; M-O. The curve of blood glucose value in ITT; P-R. The decline percentage of blood glucose at 40 min in ITT. Data are presented as mean ± SEM, n=6-8. (*P<0.05, **P<0.01, ***P<0.001 vs. LFD-*Npc1*$^{+/-}$ mice; #P<0.05, ##P<0.01 vs. HFD-*Npc1*$^{+/+}$ mice)

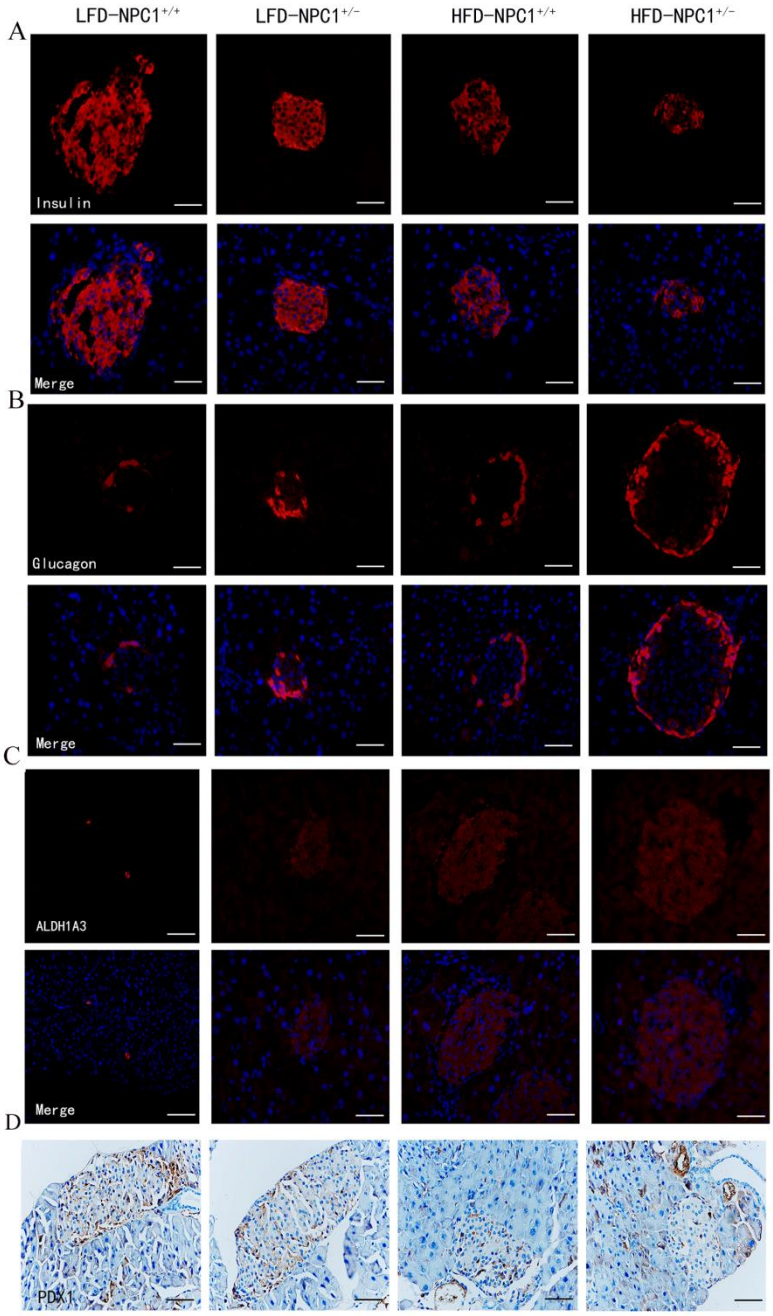

Fig 4. The functional proteins of β cells detected by immunofluorescence and immunohistochemistry.

Fig 4. The functional proteins of β cells detected by immunofluorescence and immunohistochemistry. A. Expression of Insulin; B. Expression of Glucagon; C. Expression of ALDH1A3; D. Expression of PDX1. n=3-5.

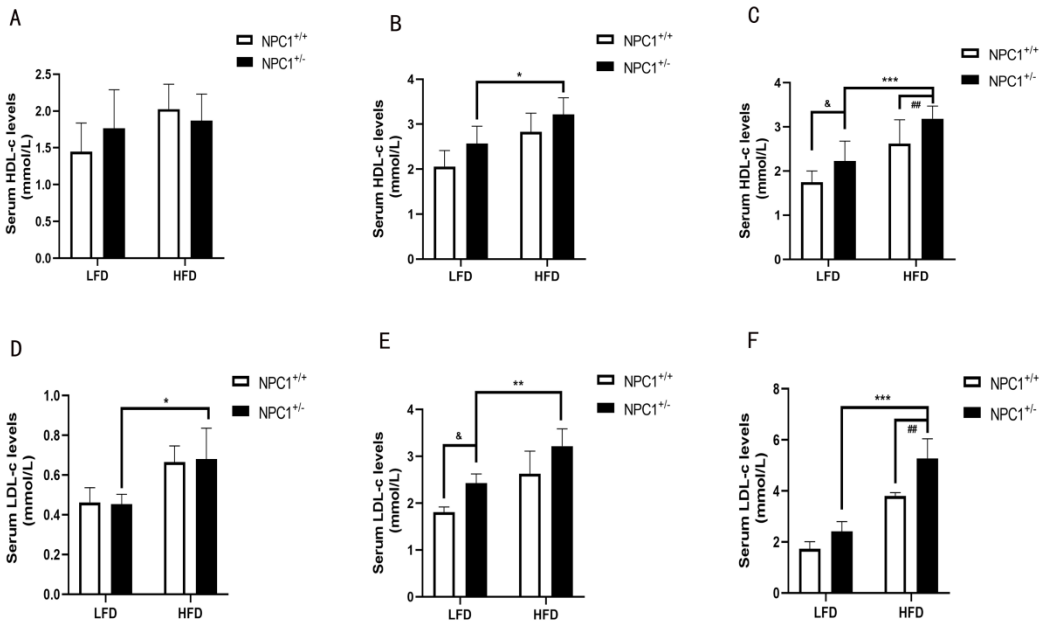

Fig S1. The continuous changes of serum HDL-c and LDL-c.

Fig S1. The continuous changes of serum HDL-c and LDL-c. A-C. serum HDL-c level after feeding HFD or LFD for 2, 4 and 6 months; D-F. serum LDL-c level after feeding HFD or LFD for 2, 4 and 6 months. n= 6-9. (*P < 0.05, **P < 0.01, ***P < 0.001 vs. LFD-*Npc1*$^{+/-}$ mice; ##P < 0.01 vs. HFD-*Npc1*$^{+/+}$ mice; &P < 0.05 vs. LFD-*Npc1*$^{+/+}$ mice).

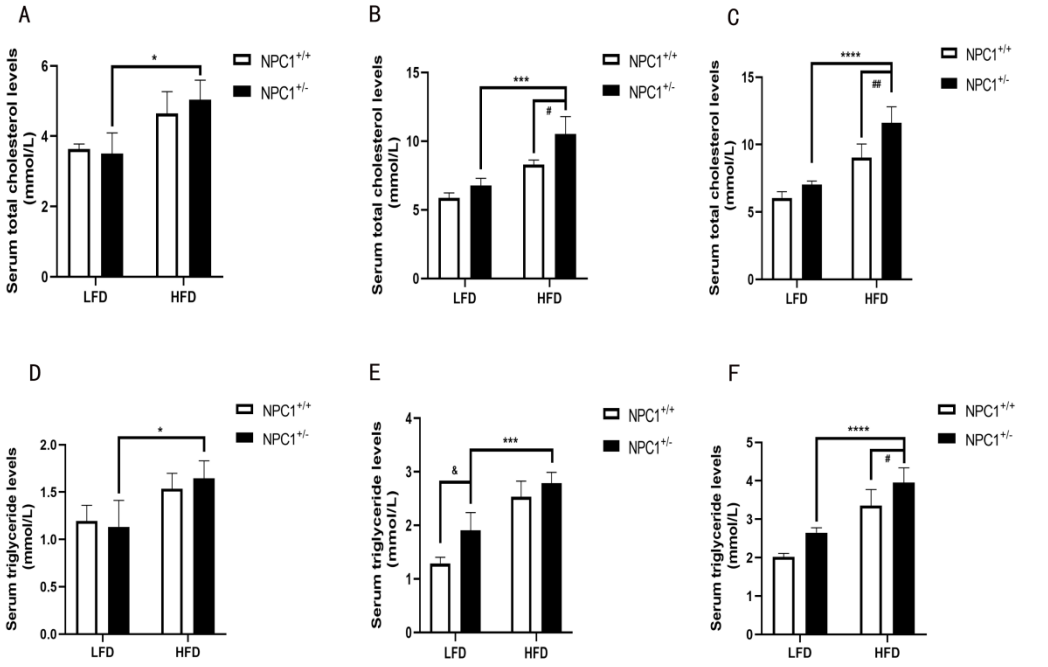

Fig S2. The continuous changes of serum TC and TG in each group.

Fig S2. The continuous changes of serum TC and TG in each group. A-C. TC in each group after feeding HFD or LFD for 2, 4 and 6 months. D-F. TG in each group after feeding HFD or LFD for 2, 4 and 6 months. n=8-10. (*P < 0.05, **P < 0.01, ***P < 0.001 vs. LFD-*Npc1*$^{+/-}$ mice; ##P < 0.01 vs. HFD-*Npc1*$^{+/+}$ mice; &P < 0.05 vs. LFD-*Npc1*$^{+/+}$ mice).

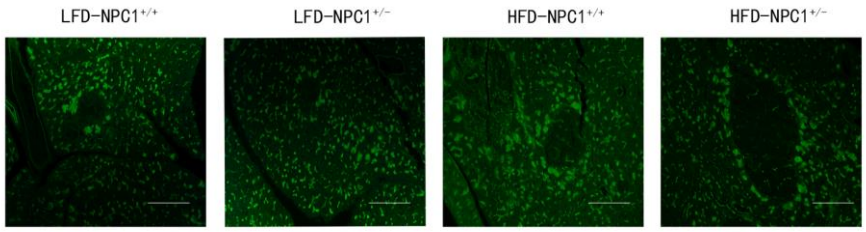

Fig S3. Thioflavin S staining of islets in each group.

Fig S3. Thioflavin S staining of islets in each group.

Discussion

The biological function of Npc1 protein is to maintain the intracellular cholesterol homeostasis by regulate the transport of cholesterol esters [2]. Homozygous mutation of *NPC1* gene can lead to loss of functions or even premature death of most cell, which is characterized by progressive and fatal neurodegeneration. *NPC1* heterozygous mutation mainly causes the disturbance of fat storage in liver and other tissues, which is characterized by abnormal accumulation of unesterified cholesterol in different degrees. According to recent epidemiological statistics, *NPC1* heterozygous mutation easily induced late obesity in adult males, and this phenomenon was closely related to the age and eating habits [18]. Related findings explored that the phenotypic and pathological changes of *Npc1*$^{+/-}$ mice fed with HFD were highly similar to those of human *NPC1* heterozygous mutation. The genome-wide association studies emphasized the significance of common *NPC1* variants in adult with obesity or type 2 diabetes [19]. In this study, male *Npc1*$^{+/-}$ mice were used as a model to investigate the effects of *NPC1* heterozygous mutation on glucolipid metabolism and islet function from the point of view of β-cell cholesterol metabolism disorder.

Our study indicated that the expression of *NPC1* decreased by 50% in C57 BALB/cJ-*Npc1*$^{+/-}$ mice, and only male *Npc1*$^{+/-}$ mice were more likely to gain body weight when fed with 60% HFD, but not with LFD, which is consistent with gene-food interaction in other studies [20]. In order to further investigate the specific relationship between NPC1 heterozygous mutation and liver dysfunction, insulin resistance and islet β-cell dysfunction, we hybridized *Npc1*$^{+/-}$ mice with wild type C57BL/6C mice and used their offspring to explore the combined effect of gene and food. With the induction of 60% HFD, male *Npc1*$^{+/-}$ mice gradually appeared abdominal obesity, accompanied by abnormal glucolipid metabolism, oral glucose intolerance, insulin resistance and hyperglycemia and other clinical manifestations of diabetes [21]. The overall results showed that high-calorie diet obviously aggravate the incidence of obesity and diabetes in male *Npc1*$^{+/-}$ mice.

As expected, the white adipose tissue and liver weight of HFD-*Npc1*$^{+/-}$ mice increased markedly compared with those of HFD-*Npc1*$^{+/+}$ and LFD-*Npc1*$^{+/-}$ groups, and HE staining showed an obvious increase in the diameter of epididymal adipocytes. Morphological examination showed liver degeneration and destruction of islet structure in HFD-*Npc1*$^{+/-}$ mice. It is worth noting that HFD-*Npc1*$^{+/-}$ mice had characteristics of fat infiltration and metabolic inflammation in liver, indicating the obvious non-alcoholic hepatitis associated with local insulin resistance and abnormal energy metabolism [22, 23]. Further detection of tissue homogenate proved the accumulation of TC and TG in liver and pancreas, showing the disorder of lipid metabolism, which may further affect the function of liver and β cells [24].

Previous studies revealed that NPC1 was expressed in many organs and had certain biological functions, yet few studies had been done on the islet function [25]. We used *NPC1* heterozygous mutated mice to further explore the effects of intra-pancreatic cholesterol accumulation on obesity and diabetes. The 50% deletion of NPC1 protein was accompanied by the accumulation of cholesterol in islets of *Npc1*$^{+/-}$ mice, which is an important factor leading to dysfunction of β cells [26]. However, we did not detect the accumulation of amyloid in islets by thioflavin S staining, the main reason may be the different amino acid sequence of amyloid polypeptide (IAPP) was different between mice and humans [27-29]. Next, we also found that cholesterol accumulation in islets inhibited the protein expression of 4E-BP1 and PS6 in mTOR pathway of HFD-*Npc1*$^{+/-}$ mice, which were the key factors determining β-cell dedifferentiation and dysfunction [30, 31]. In addition, cholesterol accumulation was associated with the decreased expression of insulin and PDX1, indicating that β-cell function began to decline. And it was also found that the expression of glucagon and ALDH1A3 in the islets were increased, indicating β cells tended to dedifferentiate into precursor cells [32, 33].

To sum up, *NPC1* heterozygous mutants in male mice combined with HFD can easily lead to obesity or diabetes. The abnormal cholesterol metabolism occurs in islets as well as in liver, which more directly inhibits the mTORC1 pathway, to promote β cells to dedifferentiate to precursor cells and decrease the ability of insulin synthesis and secretion. The interaction between *NPC1* and HFD significantly disrupts the disorder of glucolipid metabolism, which should be closely related to cholesterol accumulation in islets and liver. Meanwhile, during this study, we found that female *NPC1* mice had a high tolerance to high

calorie diet and did not show obvious symptoms of obesity and diabetes. This phenomenon may be related to hormones in female mice, which will be another direction worthy of in-depth study.

Acknowledgements
Linhai Zou, Lixia Ji are the main designers of this study. Ji Zhou performed the animal experiments. All authors read and approved the final manuscript.

Disclosure Statement
None of the authors have any potential conflicts of interest associated with this report

References

1. Brown MS, Goldstein JL (1986) A receptor-mediated pathway for cholesterol homeostasis. Science 25: 583-602.
2. Lamri A, Pigeyre M, Garver WS, Meyre D (2018) The Extending Spectrum of NPC1-Related Human Disorders: From Niemann-Pick C1 Disease to Obesity. Endocr Rev 39: 192-220.
3. Garver WS, Francis GA, Jelinek D, Shepherd G, Flynn J, et al. (2007) The National Niemann-Pick C1 disease database: report of clinical features and health problems. Am J Med Genet A 143a: 1204-1211.
4. Chen FW, Gordon RE, Ioannou YA (2005) NPC1 late endosomes contain elevated levels of non-esterified ('free') fatty acids and an abnormally glycosylated form of the NPC2 protein. Biochem J 390: 549-561.
5. Higgins ME, Davies JP, Chen FW, Ioannou YA (1999) Niemann-Pick C1 is a late endosome-resident protein that transiently associates with lysosomes and the trans-Golgi network. Mol Genet Metab 68: 1-13.
6. Naureckiene S, Sleat DE, Lackland H, Fensom A, Vanier MT, et al. (2000) Identification of HE1 as the second gene of Niemann-Pick C disease. Science 290: 2298-2301.
7. Cologna SM, Rosenhouse-Dantsker A (2019) Insights into the Molecular Mechanisms of Cholesterol Binding to the NPC1 and NPC2 Proteins. Adv Exp Med Biol 1135: 139-160.
8. Erickson RP (2018) Do GWAS and studies of heterozygotes for NPC1 and/or NPC2 explain why NPC disease cases are so rare? J Appl Genet 59: 441-447.
9. Loftus SK, Morris JA, Carstea ED, Gu JZ, Cummings C, et al. (1997) Murine model of Niemann-Pick C disease: mutation in a cholesterol homeostasis gene. Science 277: 232-235.
10. Meyre D, Delplanque J, Chèvre JC, Lecoeur C, Lobbens S, et al. (2009) Genome-wide association study for early-onset and morbid adult obesity identifies three new risk loci in European populations. Nat Genet 41: 157-159.
11. Pfeffer SR (2019) NPC intracellular cholesterol transporter 1 (NPC1)-mediated cholesterol export from lysosomes. J Biol Chem 294: 1706-1709.
12. Yu XH, Jiang N, Yao PB, Zheng XL, Cayabyab FS, et al. (2014) NPC1, intracellular cholesterol trafficking and atherosclerosis. Clin Chim Acta 429: 69-75.
13. Pentchev PG, Comly ME, Kruth HS, Patel S, Proestel M, et al. (1986) The cholesterol storage disorder of the mutant BALB/c mouse. A primary genetic lesion closely linked to defective esterification of exogenously derived cholesterol and its relationship to human type C Niemann-Pick disease. J Biol Chem 261: 2772-2777.
14. Jelinek D, Heidenreich RA, Erickson RP, Garver WS (2010) Decreased Npc1 gene dosage in mice is associated with weight gain. Obesity (Silver Spring) 18: 1457-1459.
15. Jelinek D, Millward V, Birdi A, Trouard TP, Heidenreich RA, et al. (2011) Npc1 haploinsufficiency promotes weight gain and metabolic features associated with insulin resistance. Hum Mol Genet 20: 312-321.
16. Jelinek D, Castillo JJ, Heidenreich RA, Garver WS (2015) The C57BL/6J Niemann-Pick C1 mouse model with decreased gene dosage is susceptible to increased weight gain when fed a high-fat diet: Confirmation of a gene-diet interaction. Gene 568: 112-113.
17. Liu R, Zou Y, Hong J, Cao M, Cui B, et al. (2017) Rare Loss-of-Function Variants in NPC1 Predispose to Human Obesity. Diabetes 66: 935-947.
18. Xiao J, Wang F, Liu Z, Yang C (2013) Telocytes in liver: electron microscopic and immunofluorescent evidence. J Cell Mol Med 17: 1537-1542.
19. Brunham LR, Kruit JK, Verchere CB, Hayden MR (2008) Cholesterol in islet dysfunction and type 2 diabetes. J Clin Invest 118: 403-408.
20. Heydemann A (2016) An Overview of Murine High Fat Diet as a Model for Type 2 Diabetes Mellitus. J Diabetes Res 2016: 2902351.
21. Bril F, Cusi K (2016) Nonalcoholic Fatty Liver Disease: The New Complication of Type 2 Diabetes Mellitus. Endocrinol Metab Clin North Am 45: 765-781.
22. Michael MD, Kulkarni RN, Postic C, Previs SF, Shulman GI, et al. (2000) Loss of insulin signaling in hepatocytes leads to severe insulin resistance and progressive hepatic dysfunction. Mol Cell 6: 87-97.
23. Garver WS, Jelinek D, Oyarzo JN, Flynn J, Zuckerman M, et al. (2007) Characterization of liver disease and lipid metabolism in the Niemann-Pick C1 mouse. J Cell Biochem 101: 498-516.
24. Ottinger EA, Kao ML, Carrillo-Carrasco N, Yanjanin N, Shankar RK, et al. (2014) Collaborative development of 2-hydroxypropyl-β-cyclodextrin for the treatment of Niemann-Pick type C1 disease. Curr Top Med Chem 14: 330-339.
25. Xu J, Dang Y, Ren YR, Liu JO (2010) Cholesterol trafficking is required for mTOR activation in endothelial cells. Proc Natl Acad Sci U S A 107: 4764-4769.
26. Raleigh D, Zhang X, Hastoy B, Clark A (2017) The β-cell assassin: IAPP cytotoxicity. J Mol Endocrinol 59: R121-r140.
27. Westermark P, Andersson A, Westermark GT (2011) Islet amyloid polypeptide, islet amyloid, and diabetes mellitus. Physiol Rev 91: 795-826.
28. Lyu J, Yang EJ, Head SA, Ai N, Zhang B, et al. (2018) Astemizole Inhibits mTOR Signaling and Angiogenesis by Blocking Cholesterol Trafficking. Int J Biol Sci 14: 1175-1185.
29. Head SA, Shi WQ, Yang EJ, Nacev BA, Hong SY, et al. (2017) Simultaneous Targeting of NPC1 and VDAC1 by Itraconazole Leads to Synergistic Inhibition of mTOR Signaling and Angiogenesis. ACS Chem Biol 12: 174-182.
30. Christensen AA, Gannon M (2019) The Beta Cell in Type 2 Diabetes. Curr Diab Rep 19: 81.
31. Bensellam M, Jonas JC, Laybutt DR (2018) Mechanisms of β-cell dedifferentiation in diabetes: recent findings and future research directions. J Endocrinol 236: R109-r143.
32. Zhu Y, Liu Q, Zhou Z, Ikeda Y (2017) PDX1, Neurogenin-3, and MAFA: critical transcription regulators for beta cell development and regeneration. Stem Cell Res Ther 8: 240.
33. Babu DA, Deering TG, Mirmira RG (2007) A feat of metabolic proportions: Pdx1 orchestrates islet development and function in the maintenance of glucose homeostasis. Mol Genet Metab 92: 43-55.